Predictive Power Control Strategy for a Grid-Connected 2L-VSI with Fixed Switching Frequency

Federico Gavilan, David Caballero, Sergio Toledo, Edgar Maqueda, Raul Gregor and Jorge Rodas
Laboratory of Power and Control Systems
Facultad de Ingeniería
Universidad Nacional de Asunción
Luque, Paraguay CP 2060
Email: http://www.dspyc.com.py/equipo.html

Marco Rivera
Department of Electrical Engineering
Universidad de Talca
Curicó, Chile CP 747 - 721
Email: marcoriv@utalca.cl

Ismael Araujo-Vargas
Instituto Politécnico Nacional
Escuela Superior de Ingeniería Mecánica y Eléctrica, ESIME
Culhuacan, México CP 80000
Email: iaraujo@ipn.mx

***Abstract*—In the recent years, model predictive control has been consolidated as a design strategy and an attractive alternative for the control of power electronic devices. This paper proposes an active and reactive power control strategy based on predictive control approach applied to grid-connected renewable energy systems. To accomplish this, a three-phase two-level voltage source inverter based topology is used in combination with a simple and efficient fixed-frequency modulation technique. Results based on a MATLAB/Simulink simulation environment are discussed and the most relevant characteristics of the proposed fixed-frequency predictive control approach are highlighted considering the total harmonic distortion as a figure of merit.**

***Index Terms*—Fixed-frequency modulation, power control, predictive control, renewable energy systems.**

I. Introduction

Model predictive control (MPC) has recently become a well established control technique mainly due to its fast dynamic response, conceptual simplicity and the ability to include nonlinearities and constraints in the design of the controller [1]. MPC techniques have been extensively applied with success in the field of power electronics, being the predictive current control the most popular case of study [2]. MPC uses a model of the real system, namely the "predictive model", to predict the future state evolutions, where the predictions are carried out for each of the possible switching states, to determine finally through an optimization process which of the switching states minimizes the defined cost function. The optimization is performed by exhaustive search over all possible realizations of the control action. This guarantees optimality of the results but requires a high computational cost; however, the increase in computing power of available control devices, like a digital signal controller, makes possible the implementation of the MPC approach for controlling isolated systems, micro grids or power grid-connected systems [3].

From a practical point of view the MPC strategy provides a variable switching frequency. Furthermore, one of the main drawbacks of the MPC methods are that the control can choose only from a limited number of valid switching states because of the absence of a modulator. This generates noise as well as large voltage and current ripples [4]. Moreover, the variable switching frequency produces a spread spectrum, decreasing the performance of the system in terms of power quality [5].

To address the aforementioned problems, this paper proposes a fixed switching frequency (FSF)-MPC, in order to control a three-phase two-level voltage source inverter (2L-VSI) in grid integration with a photovoltaic (PV) real system. The proposed control approach uses a suitable modulation scheme in the cost function minimization of the predictive algorithm for a selected number of switching states. With this, the duty cycles are generated for two active vectors and a zero vector which are applied to the 2L-VSI using a given switching pattern in order to obtain an efficient dynamic of the system.

The paper is organized as follows. Section II describes the design of the proposed FSF-MPC. Simulation results are then given in Section III to verify the proposed control scheme, and finally the conclusions are summarized in the last section.

II. Proposed FSF-MPC method

The 2L-VSI is one of the most widespread converter topologies found in the literature [6]. Moreover, it features a generic structure and operating principle that can be easily extended to other converter topologies. Therefore, this topology has been selected in this paper. Besides, a real $2.4\,\text{kW}$ bi-axial solar PV tracking system is considered as a distributed generation scheme for generating the voltage (V_{dc}). More details of this system can be found in [7]-[9].

The topology of a 2L-VSI is shown in Fig. 1. The switching function can be defined as $S_x \in \{1, 0\}$ where the subscript x denotes each phase ($x = a, b, c$). Given the constraint that each

978-1-5090-3794-0/16/$31.00

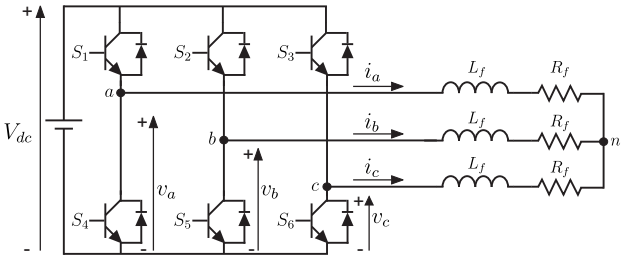

Fig. 1. Used 2L-VSI topology.

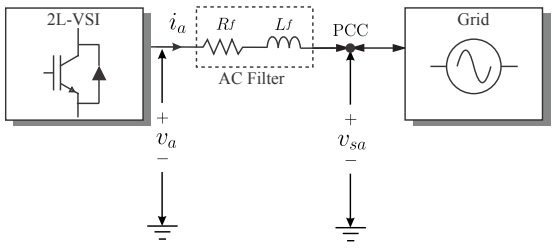

Fig. 2. Inverter and grid connection through a RL filter.

leg of two switches must operate in a complementary way for the correct operation and prevent a short circuit of the V_{dc} voltage, the switching status are defined as follows:

$$\begin{aligned} S_a &= \begin{cases} 1, & \text{if } S_1 = 1 \ \ \& \ \ S_4 = 0 \\ 0, & \text{if } S_1 = 0 \ \ \& \ \ S_4 = 1 \end{cases} \\ S_b &= \begin{cases} 1, & \text{if } S_2 = 1 \ \ \& \ \ S_5 = 0 \\ 0, & \text{if } S_2 = 0 \ \ \& \ \ S_5 = 1 \end{cases} \\ S_c &= \begin{cases} 1, & \text{if } S_3 = 1 \ \ \& \ \ S_6 = 0 \\ 0, & \text{if } S_3 = 0 \ \ \& \ \ S_6 = 1 \end{cases} \end{aligned} \tag{1}$$

The output voltage ($v_a, v_b and v_c$) can be synthesized as a function of the 2L-VSI switches and the voltage V_{dc} as:

$$\begin{aligned} v_a &= S_a V_{dc} \\ v_b &= S_b V_{dc} \\ v_c &= S_c V_{dc} \end{aligned} \tag{2}$$

A. Predictive model description

Fig. 2 shows a single-phase of a three-phase electrical filter, connected between the distributed generation system and the grid, through the point of common coupling (PCC). Applying Kirchhoff's voltage law to the scheme of Fig. 2, the system dynamics can be expressed in terms of i_a, i_b and i_c currents as follows:

$$v_x - v_{sx} - R_f i_x = L_f \frac{di_x}{dt} \tag{3}$$

where v_x is the 2L-VSI output voltage, v_{sx} is the grid voltage and i_x is the current output; the subscript x denotes each phase ($x = a, b, c$). R_f and L_f are the filter resistance and inductance, respectively.

To simplify the analysis, a stationary reference frame ($\alpha - \beta$) transformation is used [10]. Then, (1), (2) and (3) can be expressed by means of:

$$v_\alpha - v_{s\alpha} - R_f i_\alpha = L_f \frac{di_\alpha}{dt} \tag{4}$$

$$v_\beta - v_{s\beta} - R_f i_\beta = L_f \frac{di_\beta}{dt} \tag{5}$$

where $v_{s\alpha}$ and $v_{s\beta}$ are the grid voltages, v_α and v_β are the 2L-VSI output voltage in the stationary reference frame.

The derivative of the current can be replaced by the first-order forward-Euler approximation method:

$$\frac{di}{dt} \approx \frac{i(k+1) - i(k)}{T_s} \tag{6}$$

where T_s is the sampling time. By applying (6) in (4) and (5), the predictions of the state vector for the sample $k+1$, namely $i_\alpha^p(k+1)$ and $i_\beta^p(k+1)$, can be written as:

$$i_\alpha^p(k+1) = \left(1 - \frac{R_f T_s}{L_f}\right) i_\alpha(k) + \frac{T_s}{L_f}[v_\alpha(k) - v_{s\alpha}(k)] \tag{7}$$

and

$$i_\beta^p(k+1) = \left(1 - \frac{R_f T_s}{L_f}\right) i_\beta(k) + \frac{T_s}{L_f}[v_\beta(k) - v_{s\beta}(k)] \tag{8}$$

respectively.

B. Cost function definition

The cost function should include all terms that will be optimized. In current control, the most important figure is the tracking error in the predicted currents for the next sample as follows:

$$J(k+1) = \| \, e_{i\alpha}(k+1) \, \|^2 + \| \, e_{i\beta}(k+1) \, \|^2 \tag{9}$$

where

$$\begin{aligned} \| \, e_{i\alpha}(k+1) \, \| &= \| \, i_\alpha^*(k+1) - i_\alpha^p(k+1) \, \| \\ \| \, e_{i\beta}(k+1) \, \| &= \| \, i_\beta^*(k+1) - i_\beta^p(k+1) \, \| \end{aligned}$$

$\| \, . \, \|$ denotes vector magnitude, $i_{\alpha\beta}^*(k+1)$ and $i_{\alpha\beta}^p(k+1)$ are vectors which contain the reference and the prediction currents, respectively.

C. Reference generation

Active and reactive power references in current terms are shown as follows [11]:

$$i_\alpha^*(k+1) = \frac{2}{3} \frac{v_{s\alpha}(k)}{v_{s\alpha}^2(k) + v_{s\beta}^2(k)} P^* + \frac{2}{3} \frac{v_{s\beta}(k)}{v_{s\alpha}^2(k) + v_{s\beta}^2(k)} Q^* \tag{10}$$

and

$$i_\beta^*(k+1) = \frac{2}{3} \frac{v_{s\beta}(k)}{v_{s\alpha}^2(k) + v_{s\beta}^2(k)} P^* - \frac{2}{3} \frac{v_{s\alpha}(k)}{v_{s\alpha}^2(k) + v_{s\beta}^2(k)} Q^* \tag{11}$$

being P^* and Q^* the active and reactive power references, respectively.

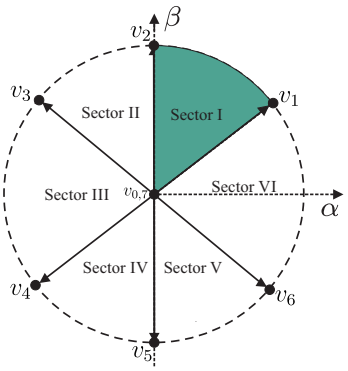

Fig. 3. Avalaible sectors for the 2L-VSI.

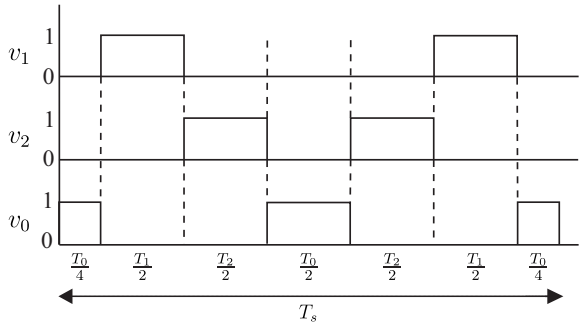

Fig. 4. Switching pattern for the optimal vectors.

D. Proposed predictive-fixed control technique

In space vector modulation, it is possible to define each available vector for the 2L-VSI in the $(\alpha - \beta)$ plane as shown in Fig. 3. Are defined six sectors which are given by two adjacent vectors, being the first sector the one between vector v_1 and vector v_2, as shown in Fig. 3. Moreover the proposed technique evaluates the prediction of the two active vectors that conform each sector at every sampling time and evaluates the cost function separately for each prediction. The cost function, defined by (9), is evaluated for each case. For example, for sector I, the first prediction and cost function J_1 is evaluated for vector v_1 and the second prediction and cost function J_2 is evaluated for vector v_2. Each prediction is evaluated based on (7) and (8), and the only change is in respect to the calculation of the 2L-VSI output voltage. The duty cycles for the two active vectors are calculated by solving the following equations:

$$d_i = \frac{\delta}{J_i} \tag{12}$$

were δ is the constant of proportionality, the subscript i denotes the adjacent vectors ($i = 1, 2$) and $i = 0$ corresponds to the duty cycle of a zero vector which is evaluated only one time.

$$d_0 + d_1 + d_2 = T_s \tag{13}$$

By solving (12) and (13) is possible to obtain the value of δ and the duty cycles for each vector are given as:

$$d_0 = \frac{T_s J_1 J_2}{J_0 J_1 + J_1 J_2 + J_0 J_2} \tag{14}$$

$$d_1 = \frac{T_s J_0 J_2}{J_0 J_1 + J_1 J_2 + J_0 J_2} \tag{15}$$

$$d_2 = \frac{T_s J_0 J_1}{J_0 J_1 + J_1 J_2 + J_0 J_2} \tag{16}$$

Considering these expressions, the new cost function, which is evaluated at every sampling time, is defined as:

$$g(k+1) = d_1 J_1 + d_2 J_2 \tag{17}$$

The two vectors that minimize (17) and the zero vector are selected and applied to the 2L-VSI at the next sampling time. After obtaining the duty cycles and selecting the optimal two vectors to be applied, is defined the time that each vector will be applied, such as [12]:

$$\begin{aligned} T_0 &= T_s d_0 \\ T_1 &= T_s d_1 \\ T_2 &= T_s d_2 \end{aligned} \tag{18}$$

A switching pattern procedure, such as the one shown in Fig. 4, is adopted with the goal of applying the two active vectors and one zero vector [13].

E. Optimization procedure

An exhaustive search over all possible realizations of the control actions is performed. The search space given by the set of possible vectors can be defined as $\varepsilon = 6$, were ε is the number of sectors. The optimization algorithm selects the optimum vector S^{opt} which minimizes the cost function g, as detailed in Algorithm 1.

Algorithm 1 Optimization algorithm

1. Initialize $J_{opt} := \infty, i := 1$
2. Compute predictive currents for zero vector Eqn. (7) & (8)
3. Compute the cost function J_0 Eqn. (9)
4. **while** $i \leq \varepsilon$ **do**
5. Compute output voltages Eqn. (2) for vector v_1
6. Compute the predictive currents Eqn. (7) & (8) for v_1
7. Compute the cost function J_1 Eqn. (9)
8. Compute output voltages Eqn. (2) for vector v_2
9. Compute the predictive currents Eqn. (7) & (8) for v_2
10. Compute the cost function J_2 Eqn. (9)
11. Compute the duty cycles Eqn. (14) & (15) & (16)
12. Compute the cost function g Eqn. (17)
13. **if** $g < J_{opt}$ **then**
14. $J_{opt} \leftarrow g$, $S^{opt} \leftarrow S_i$
15. $i = i + 1$
16. **end while**
17. Apply the duty cycles for the optimum vector S^{opt}

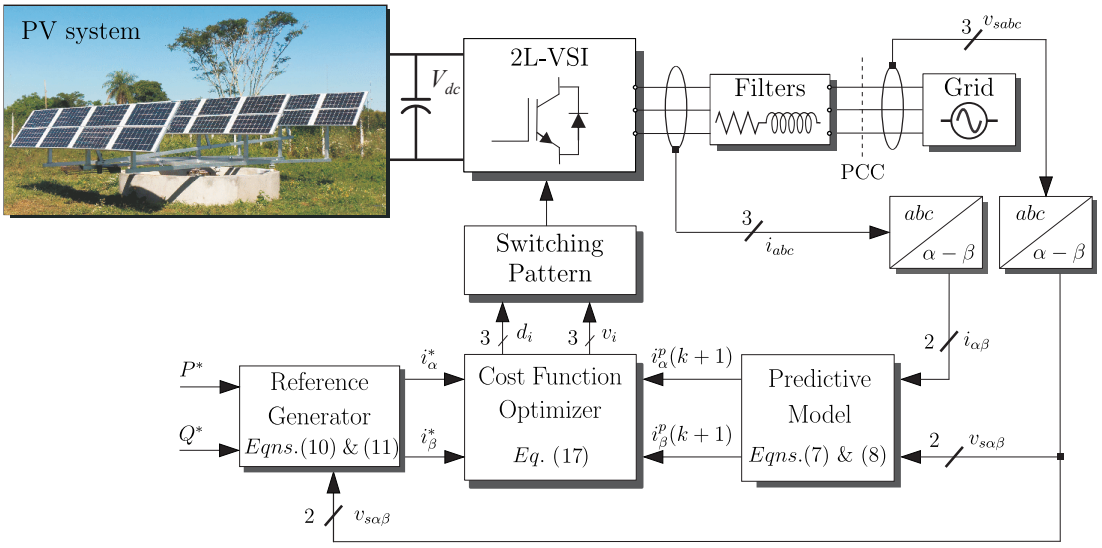

Fig. 5. Configuration of a grid-connected system with a 2L-VSI.

III. Simulation Results and Discussion

The 2L-VSI has been modeled in MATLAB/Simulink to validate the proposed control scheme, considering the electrical parameters that are shown in Table I. Simulations have been performed to show the accuracy of the proposed controller. Results were carried out in both, steady and transient states conditions. Numerical integration by means of the first-order forward-Euler method has been applied to obtain the evolution of the controlled variables over a horizon of prediction time. A detailed block diagram of the proposed predictive current control technique is provided in Fig. 5.

A. Transient condition analysis

To demonstrate the performance of the proposed strategy in terms of dynamic response, transient state analysis was done. Fig. 6 (zoom) shows the step changes in the active power reference P^*, from $2,400$ W to $1,500$ W at the instant $t = 0.06$ s, and for $1,500$ W to $1,000$ W at $t = 0.12$ s. In both cases it is observed a very good dynamic response, with a settling times of $ts = 0.005$ s, which represents a quarter of the grid cycle.

TABLE I
Electrical Parameters

PARAMETER	SYMBOL	VALUE	UNIT
Electrical signal frequency	f_s	50	Hz
Grid voltage signal amplitude	V_s	220	V
Filter resistance	R_f	2.3	Ω
Filter inductance	L_f	30	mH
Inverter switching period	T_s	50	μs
Active power reference	P^*	$2,400$	W
Reactive power reference	Q^*	0	VAR

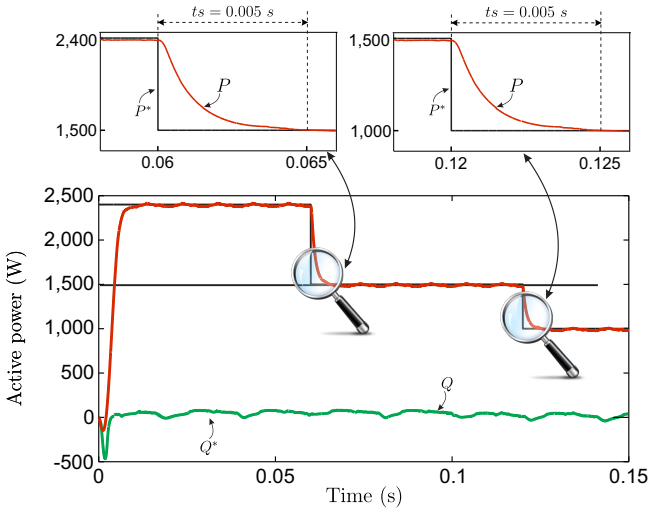

Fig. 6. Simulation results of the dynamic response. Active power reference *vs.* simulated.

B. Steady-state analysis

Fig. 6 also shows simulation results in steady-state for the proposed FSF-MPC control approach. The active power reference was initially set to 2,400 W and after $t = 0.06$ s, the value of the active power reference was changed to $1,500$ W. Besides, at $t = 0.12$ s the active power value was set to $1,000$ W. In the three cases studied above it is observed a very good tracking of the active power P to its respective references P^*. Furthermore, the reactive power Q follows the reference Q^* and it remains constant in the order that was set $Q^* = 0$ VAR. As mentioned in the previous section, the active and reactive power references can be expressed in current terms in the stationary reference frame $(\alpha-\beta)$. Behaviour of the current at the PCC are shown in Fig. 7. It can be appreciated that the currents fluctuate slightly due to the switching electronic

TABLE II
THD ANALYSIS

VARIABLES	$P^* = 2,400$ W	$P^* = 1,500$ W	$P^* = 1,000$ W
i_α	1.69 %	2.81 %	4.31 %
i_β	1.60 %	2.44 %	3.73 %

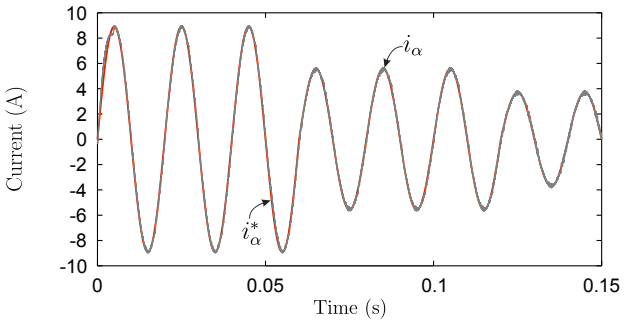

Fig. 7. Tracking current in stationary reference.

components of the 2L-VSI, generating a small distortion. Total harmonic distortion (THD) of the currents is used to evaluate the performance of the proposed control technique. Table II shows the THD analysis of currents i_α and i_β for the three power references studied, in all cases values below 5% were obtained. It is important to highlight that to have a similar THD value in the classical MPC method it is necessary a higher sampling time with respect to the proposed method. On the other hand, the 2L-VSI voltage output switching pattern is shown in Fig. 8. It is noted as the adjacent vectors and the zero vector applied to 2L-VSI during a sampling period exhibit the proposed sequence.

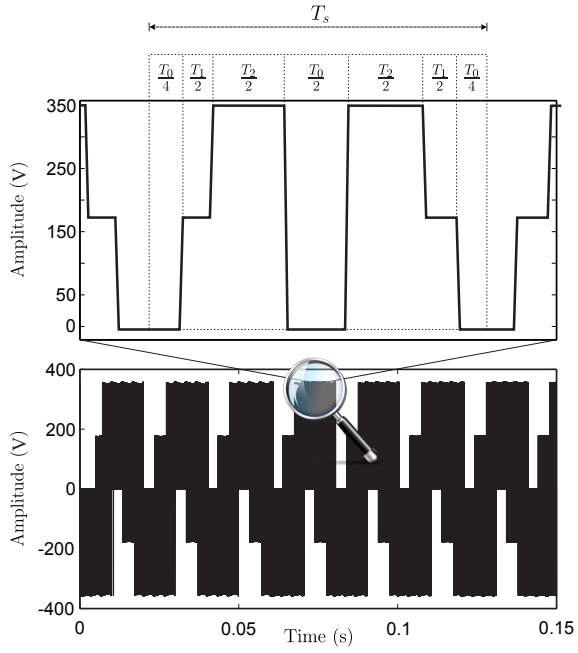

Fig. 8. Switching pattern of the output voltage.

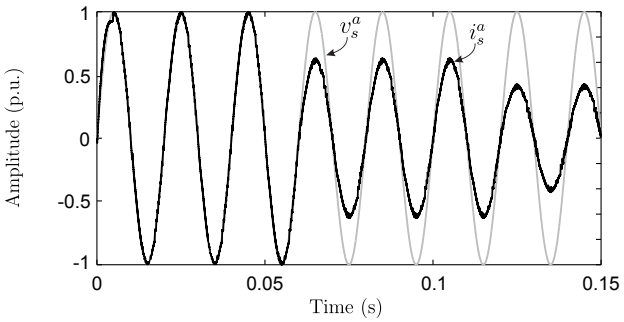

Fig. 9. Current and voltage behaviour at the output.

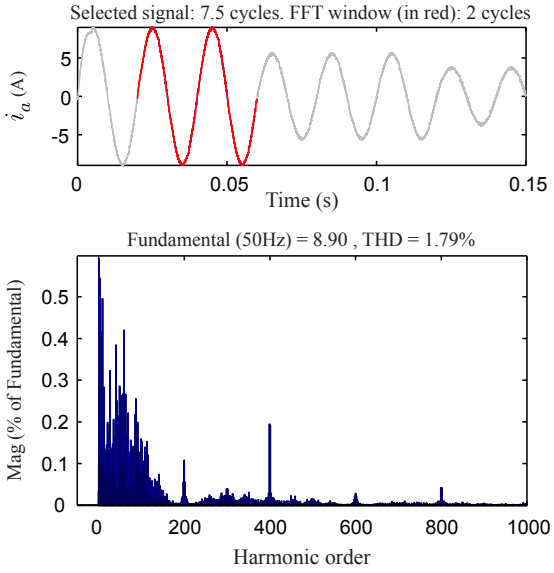

Fig. 10. Current output i_a THD.

Current and voltage behaviour at the output are shown in Fig. 9 for each of the three powers references mentioned in the previous section. When the reference power decreases, the current amplitude decreases, keeping constant the voltage value. Finally, Fig. 10 show the THD for the i_a current. Similar results were obtained for b and c phases.

IV. Conclusions

This paper introduced a power control technique for grid-connected applications by using a predictive-fixed current control for a 2L-VSI. The algorithm considers each of the 6 possible sectors and selects the state which minimizes a cost function. Thus, the optimal vector is applied to the 2L-VSI producing modulated sinusoidal voltage and current outputs perfectly in phase with the grid. A Matlab/Simulink model was employed to validate the proposed control method. Good accuracy level was observed (THD lower than 5 %), as well as a fast dynamic response (convergence in less than 0.005 s). The obtained results show the feasibility of the implementation of the proposed control technique, as well as its application to grid-connected systems.

ACKNOWLEDGMENT

The authors would like to thank the Paraguayan Government for the economical support they provided by means of a CONACYT grant (project 14-INV-097). This work was also founded by FONDECYT Regular Project No. 1160690. Additionally, the authors would like to thank the National Council of Science and Technology of Mexico (CONACyT Mexico) and the Instituto Politécnico Nacional (IPN) of Mexico for their encouragement and kind economic support.

REFERENCES

[1] S. Kouro, M.A. Perez, J. Rodriguez, A.M. Llor, and H.A. Young, "Model Predictive Control: MPC's Role in the Evolution of Power Electronics," *IEEE Ind. Electron. Mag.*, vol. 9, no. 4, pp. 8–21, 2015.

[2] S. Vazquez, J. Leon, L.G. Franquelo, J. Rodriguez, H. Young, A. Marquez, and P. Zanchetta, "Model Predictive Control: a Review of its Applications in Power Electronics," *IEEE Ind. Electron. Mag.*, vol. 8, no. 1, pp. 16–31, 2014.

[3] D. Caballero, F. Gavilán, R. Gregor, J. Rodas, S. Toledo, and J. Rodriguez-Pineiro, "MBPC Power Control in Three-Phase Inverters for Grid-Connected Applications," in *Proc. ISGT LATAM*, Montevideo, Uruguay, 2015, pp. 817–821.

[4] R. Gregor, J. Rodas, J. Munoz, D. Gregor, M. Ayala, and O. Gonzalez, "Predictive-Fixed Switching Frequency Technique for 5-Phase Induction Motor Drives," in *Proc. SPEEDAM*, Capri, Italy, 2016, pp. 761–767.

[5] J. Rodriguez, M.P. Kazmierkowski, J.R. Espinoza, P. Zanchetta, H. Abu-Rub, H. A. Young, and C.A. Rojas, "State of the Art of Finite Control Set Model Predictive Control in Power Electronics," *IEEE Trans Ind. Informatics*, vol. 9, no. 2, pp. 1003–1016, 2013.

[6] E. Levi, "Advances in Converter Control and Innovative Exploitation of Additional Degrees of Freedom for Multiphase Machines," *IEEE Trans. Ind. Electron.*, vol. 63, no. 1, pp. 433–448, 2016.

[7] R. Gregor, Y. Takase, J. Rodas, L. Carreras, D. Gregor, and A. López, "Bi-Axial Solar Tracking System Based on the MPPT Approach Integrating ICTs for Photovoltaic Applications," *Int. J. Photoenergy*, vol. 2015, Article ID 202986, 10 pages, 2015.

[8] R. Gregor, Y. Takase, J. Rodas, L. Carreras, A. López and M. Rivera, "A Novel Design and Automation of a Biaxial Solar Tracking System for PV Power Applications," in *Proc. IEEE IECON*, Vienna, Austria, 2013, pp. 1484–1489.

[9] R. Gregor, Y. Takase, J. Rodas, L. Carreras, A. López, and D. Gregor, "Integration of ICTs in a Bi-Axial Solar Tracking System for Photovoltaic Application," in *Proc. WMSCI*, Orlando, USA, 2015.

[10] G. Andreta, S. Ortmann, and L. Heldwein, "Hybrid Current Control Technique Applied to Grid Connected Inverters," in *Proc. ICIT*, Seville, Spain, 2015, pp. 2268–2274.

[11] Y. Song, and H. Nian, Stationary Frame Control Strategy for Voltage Source Inverter under Unbalanced and Distorted Grid Voltage," in *Proc. ECCE*, Pittsburgh, USA, 2014, pp. 1167–1173.

[12] M. Rivera, M. Perez, C. Baier, J. Munoz, V. Yaramasu, B. Wu, L. Tarisciotti, P. Zanchetta, and P. Wheeler, "Predictive Current Control with Fixed Switching Frequency for an NPC Converter," in *Proc. ISIE*, Rio de Janeiro, Brazil, 2015, pp. 1034–1039.

[13] M. Rivera, F. Morales, C. Baier, J. Munoz, L. Tarisciotti, P. Zanchetta, and P. Wheeler, "A Modulated Model Predictive Control Scheme for a Two-Level Voltage Source Inverter," in *Proc. ICIT*, Seville, Spain, 2015, pp. 2224–2229.